DALTON
FULL PAPER

Alkali metal–1-azaallyl complexes: X-ray crystallographic, NMR spectroscopic and *ab initio* calculational studies

David R. Armstrong,[a] William Clegg,[b] Lorraine Dunbar,[c] Stephen T. Liddle,[b] Murray MacGregor,[a] Robert E. Mulvey,*[a] David Reed[d] and Susan A. Quinn[a]

[a] *Department of Pure and Applied Chemistry, University of Strathclyde, Glasgow, UK G1 1XL. E-mail: R.E.Mulvey@Strath.ac.uk*
[b] *Department of Chemistry, University of Newcastle, Newcastle-upon-Tyne, UK NE1 7RU*
[c] *University Chemical Laboratory, Lensfield Road, Cambridge, UK CB2 1EW*
[d] *Department of Chemistry, University of Edinburgh, Edinburgh, UK EH9 3JJ*

Received 16th July 1998, Accepted 20th August 1998

A series of alkali metal–1-azaallyl complexes, [{$CH_3CH_2CH_2C(H)C(Bu^t)N(H)Li\cdot HMPA\}_2$] **1**, [{$CH_3CH_2CH_2$-$C(H)C(Bu^t)N(H)Na\cdot 2HMPA\}_2$] **2** and [{$CH_2C(Bu^t)N(H)Li\cdot HMPA\}_2$] **3**, has been synthesised by treating each appropriate metal alkyl reagent (*n*-butyllithium, *n*-butylsodium or methyllithium, respectively) with *tert*-butyl cyanide in the presence of the Lewis base HMPA [hexamethylphosphoramide, $(Me_2N)_3P{=}O$]. X-Ray crystallographic studies have established that each structure is dimeric and built around a precisely or approximately centrosymmetric rhomboidal $(N–M)_2$ ring. However, the nature of the azaallyl–metal bonding differs with **1** and **2** displaying a terminal η^1-N arrangement, while **3** displays a chelating η^3-NCC arrangement. ^{1}H and ^{13}C NMR spectroscopic studies suggest that these distinct bonding modes are retained in [$^2H_8$]toluene solution. Long-range (^4J) "W" coupling (2.4 Hz) is observed for **3** between the N*H* and one of the α-CH_2 protons, consistent with the *trans* orientation of the NH and C⋯C linkages seen in the solid state. The preference for this geometry is confirmed by *ab initio* MO calculations on models of **3**, which examine the energetics of the ketimide–azaallyl isomerism involved in the formation of **1**–**3**.

Previously we reported that lithium and sodium ketimides having a *n*-butyl substituent attached to the imido C centre undergo a 1,3-sigmatropic rearrangement to azaallyl formulations [eqn. (1)].[1] This process, which is mediated by the strong Lewis

$$CH_3CH_2CH_2CH_2(Bu^t)C{=}NM \xrightarrow{HMPA} CH_3CH_2CH_2C(H)\cdots C(Bu^t)\cdots N(H)M\cdot x\text{HMPA} \quad (1)$$
$$M = Li,\ x = 1;\ M = Na,\ x = 2$$

base HMPA, was elucidated solely on the basis of ^{1}H NMR spectroscopic evidence in solution. No information on the structural nature of the metal azaallyl products or on the extent of delocalisation within the NCC moiety was obtained at that time. Of interest because of their isoelectronic relationship to carboxylato and allyl ligands, the ligands in these alkali metal complexes are 1-azaallyl, which in general have received considerably less attention than other nitrogen pseudo-allyl systems such as amidates and amidinates.[2–4] Since the publication of our original communication a related ketimide to azaallyl transformation involving the migration of an $SiMe_3$ group rather than a H atom has been reported [eqn. (2)], though the

$$2(Me_3Si)_2CHLi + 2Bu^tC{\equiv}N \longrightarrow \text{"}2(Me_3Si)_2CH(Bu^t)C{=}NLi\text{"} \xrightarrow{\text{Diethyl ether}} [\{(Me_3Si)C(H)\cdots C(Bu^t)\cdots N(SiMe_3)Li\}_2] \quad (2)$$

intermediate ketimide was not actually identified but merely postulated to exist.[5,6] The α,ω-bis(trimethylsilyl)-1-azaallyl product was structurally characterised and shown to be a η^3-dimer with the metal binding to all three atoms in the delocalised NCC anion.[7,8] Lappert *et al*. have since shown that this compound is effective as a ligand transfer reagent in the preparation of copper(I) 1-azaallyls.[9]

To provide a comparison with this solvent-free trimethylsilyl analogue, and to establish the bonding character (imidoalkyl $[RC(H)C(Bu^t){=}NH]^-$ or enamido $[RC(H){=}C(Bu^t)NH]^-$) of their azaallyl anions, we have now determined the crystal structures of two HMPA solvates. These structures are presented herein, along with that of the methyl-derived analogue [{$CH_2\cdots C(Bu^t)\cdots N(H)Li\cdot HMPA\}_2$], the synthesis of which proves that other imido-C substituents containing α-C–H bonds [in this case the methyl group of $CH_3(Bu^t)C{=}NLi$] can undergo the same H-migration process in the presence of HMPA. The three complexes have also been characterised by ^{1}H and ^{13}C NMR spectroscopic studies in solution. *Ab initio* MO calculations have also been carried out to shed light on the energetics of the ketimide–azaallyl isomerism.

Results and discussion

All three azaallyl complexes [{$CH_3CH_2CH_2C(H)C(Bu^t)N(H)$-$Li\cdot HMPA\}_n$] **1**, [{$CH_3CH_2CH_2C(H)C(Bu^t)N(H)Na\cdot 2HMPA\}_n$] **2** and [{$CH_2C(Bu^t)N(H)Li\cdot HMPA\}_n$] **3** were prepared in a similar straightforward manner. Starting from *tert*-butyl cyanide and the appropriate metal alkyl reagent, a nitrile insertion reaction was carried out to generate a metal ketimide intermediate which, on treatment with HMPA *in situ*, rearranges to its azaallylic isomeric form [eqn. (3)]. The metal centres

$$RCH_2M + Bu^tC{\equiv}N \longrightarrow RCH_2(Bu^t)C{=}NM \longrightarrow RC(H)C(Bu^t)N(H)M\cdot x\text{HMPA} \quad (3)$$

involved end up solvated by HMPA molecules: two per Na centre and one per Li centre.

X-Ray crystallographic studies

Each azaallyl complex is found to be dimeric ($n = 2$) in the crystal (Figs. 1–3). Dimerisation is accomplished through a central $(NM)_2$ planar ring, the amide substituents of which are

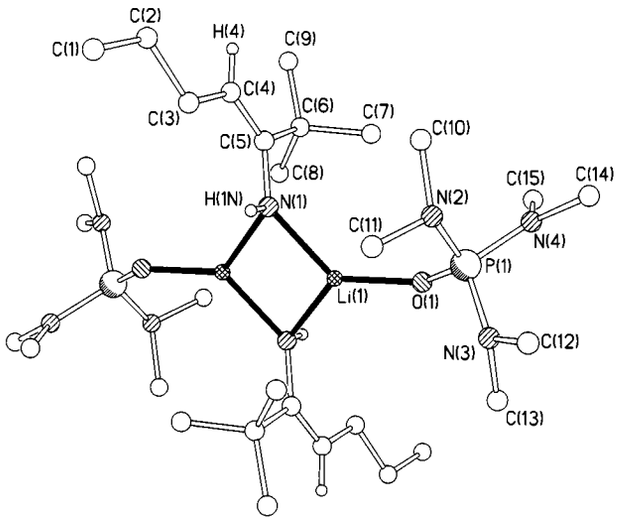

Fig. 1 Molecular structure of **1** showing the atom-labelling scheme. Hydrogen atoms attached to the azaallyl NCC unit are included; others are omitted for clarity.

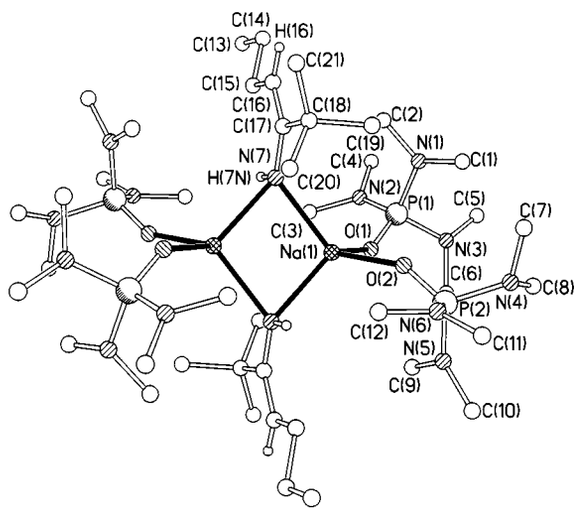

Fig. 2 Molecular structure of **2** showing the atom-labelling scheme. Hydrogen atoms attached to the azaallyl NCC unit are included; others are omitted for clarity.

disposed in a transoid conformation. Terminally bound HMPA solvent ligands complete the structures. While in terms of these gross structural features the three complexes appear to belong to the same family, an analysis of dimensions reveals a more accurate discriminating picture: elaborating, complexes **1** and **2** (Figs. 1 and 2, respectively) are best described as η^1-N azaallyl systems, in contrast to complex **3** which is a η^3-NCC alternative (Fig. 3). Selected dimensions for each complex are given in Tables 1–3. From this information it is discernible that in **1** only the N terminus of the NCC unit binds to the Li^+ cations, at a mean distance of 2.012 Å; the C(5)···Li(1) and C(4)···Li(1) separation distances are substantially longer and non-bonding at 2.947 and 3.929 Å, respectively. In **3**, however, the corresponding C atoms C(5)/C(6) and C(17)/C(18) form close contacts with the Li^+ cation in the range 2.361–2.526 Å, the shortest of which involve the central NCC atoms. Furthermore, its $(NLi)_2$ planar ring is much more asymmetrical than that in **1** with two short and two long N–Li edges (mean lengths, 1.991 and 2.055 Å respectively). In view of these considerations, **3** is best regarded as a composite of two monomeric fragments C(6)C(5)N(1)Li(2) and C(18)C(17)N(5)Li(1) which exhibit η^3-NCC ⟶ Li π-interactions (a monomer of this type is also implicated by the *ab initio* MO study; see below). The near-orthogonal C(17)N(5)Li(1) and C(5)N(1)Li(2) bond angles [84.35(19) and 85.9(2)°, respectively; *cf*. the obtuse values of

Table 1 Selected bond lengths (Å) and angles (°) for compound **1**

Li(1)–N(1)	2.008(4)	Li(1)–N(1A)	2.016(4)
Li(1)–O(1)	1.851(4)	O(1)–P(1)	1.4772(16)
N(1)–C(5)	1.390(3)	C(1)–C(2)	1.524(3)
C(2)–C(3)	1.511(3)	C(3)–C(4)	1.498(3)
C(4)–C(5)	1.345(3)	C(5)–C(6)	1.538(3)
O(1)–Li(1)–N(1)	128.2(2)	O(1)–Li(1)–N(1A)	128.3(2)
N(1)–Li(1)–N(1A)	103.41(18)	C(5)–N(1)–Li(1)	135.43(19)
C(5)–N(1)–Li(1A)	118.67(18)	Li(1)–N(1)–Li(1A)	76.59(18)
P(1)–O(1)–Li(1)	137.30(15)	C(4)–C(5)–N(1)	124.7(2)
C(4)–C(5)–C(6)	121.74(19)	N(1)–C(5)–C(6)	113.56(18)

Symmetry transformations used to generate equivalent atoms: A $-x$, $-y+1$, $-z+1$.

Table 2 Selected bond lengths (Å) and angles (°) for compound **2**

Na(1)–N(7)	2.3902(17)	Na(1)–N(7A)	2.4305(17)
Na(1)–O(1)	2.2801(14)	Na(1)–O(2)	2.2589(15)
O(1)–P(1)	1.4823(13)	O(2)–P(2)	1.4724(14)
N(7)–C(17)	1.364(2)	C(13)–C(14)	1.514(3)
C(14)–C(15)	1.521(3)	C(15)–C(16)	1.493(3)
C(16)–C(17)	1.369(2)	C(17)–C(18)	1.539(3)
O(2)–Na(1)–O(1)	100.51(6)	O(2)–Na(1)–N(7)	119.71(6)
O(1)–Na(1)–N(7)	111.45(6)	O(2)–Na(1)–N(7A)	101.30(6)
O(1)–Na(1)–N(7A)	126.82(6)	N(7)–Na(1)–N(7A)	98.35(5)
C(17)–N(7)–Na(1)	133.42(13)	C(17)–N(7)–Na(1A)	129.20(12)
Na(1)–N(7)–Na(1A)	81.65(5)	P(1)–O(1)–Na(1)	140.08(8)
P(2)–O(2)–Na(1)	149.96(8)	N(7)–C(17)–C(16)	125.55(18)
N(7)–C(17)–C(18)	114.28(16)	C(16)–C(17)–C(18)	120.10(16)

Symmetry transformations used to generate equivalent atoms: A $-x+2$, $-y$, $-z+2$.

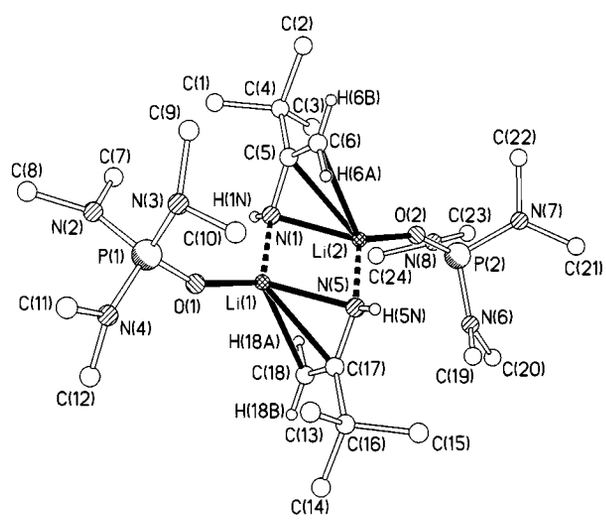

Fig. 3 Molecular structure of **3** emphasising the η^3-NCC–Li bonded monomeric fragments within the dimeric arrangement, and showing the atom-labelling scheme. Hydrogen atoms attached to the azaallyl NCC unit are included; others are omitted for clarity.

118.67(18) and 135.43(19)° for the corresponding bond angles in **1**] support this interpretation. This geometry allows the sterically accessible open edges of both monomeric fragments to approach each other closely in a transoid manner, and to join together through short N(1)–Li(1) and N(5)–Li(2) bonds. These bonds possess more σ-character, as gauged by the near-planarity of the C(6)C(5)N(1)Li(1) and C(18)C(17)N(5)Li(2) units (root-mean-square deviations 0.055 and 0.044 Å), than the N(5)–Li(1) and N(1)–Li(2) bonds which are inclined at angles of 56.1 and 55.0° respectively to their NCC azaallyl planes indicative of a high degree of π-character. Note that in order to effect the η^3-NCC–Li interaction the N–H bonds lie *trans* with respect to the delocalised C–C units, whereas a *cis* conformation marks the η^1-arrangement found in **1**. However,

Table 3 Selected bond lengths (Å) and angles (°) for compound **3**

Li(1)–N(1)	1.999(5)	Li(1)–N(5)	2.066(5)
Li(1)–O(1)	1.846(5)	Li(1)–C(17)	2.361(5)
Li(1)–C(18)	2.515(5)	Li(2)–N(5)	1.982(5)
Li(2)–N(1)	2.043(5)	Li(2)–O(2)	1.864(5)
Li(2)–C(5)	2.371(5)	Li(2)–C(6)	2.526(5)
O(1)–P(1)	1.4732(18)	O(2)–P(2)	1.4744(18)
C(4)–C(5)	1.541(4)	C(5)–C(6)	1.361(4)
C(5)–N(1)	1.359(3)	C(16)–C(17)	1.544(4)
C(17)–C(18)	1.354(3)	C(17)–N(5)	1.364(3)
O(1)–Li(1)–N(1)	122.1(2)	O(1)–Li(1)–N(5)	126.6(3)
N(1)–Li(1)–N(5)	102.1(2)	O(1)–Li(1)–C(17)	117.7(2)
N(1)–Li(1)–C(17)	120.3(2)	N(5)–Li(1)–C(17)	35.10(10)
O(1)–Li(1)–C(18)	124.7(2)	N(1)–Li(1)–C(18)	104.3(2)
N(5)–Li(1)–C(18)	60.92(14)	C(17)–Li(1)–C(18)	32.04(10)
O(2)–Li(2)–N(5)	124.6(2)	O(2)–Li(2)–N(1)	124.0(2)
N(5)–Li(2)–N(1)	103.5(2)	O(2)–Li(2)–C(5)	115.1(2)
N(5)–Li(2)–C(5)	120.2(2)	N(1)–Li(2)–C(5)	34.87(11)
O(2)–Li(2)–C(6)	122.7(2)	N(5)–Li(2)–C(6)	103.5(2)
N(1)–Li(2)–C(6)	60.98(14)	C(5)–Li(2)–C(6)	32.06(10)
C(5)–N(1)–Li(1)	121.9(2)	C(5)–N(1)–Li(2)	85.9(2)
Li(1)–N(1)–Li(2)	77.29(19)	C(17)–N(5)–Li(2)	123.5(2)
C(17)–N(5)–Li(1)	84.35(19)	Li(2)–N(5)–Li(1)	77.11(19)
P(1)–O(1)–Li(1)	155.39(18)	P(2)–O(2)–Li(2)	158.03(18)
N(1)–C(5)–C(6)	120.0(3)	N(1)–C(5)–C(4)	119.3(2)
C(6)–C(5)–C(4)	120.6(2)	N(1)–C(5)–Li(2)	59.24(17)
C(6)–C(5)–Li(2)	80.27(19)	C(4)–C(5)–Li(2)	130.1(2)
C(5)–C(6)–Li(2)	67.67(18)	C(18)–C(17)–N(5)	120.1(2)
C(18)–C(17)–C(16)	121.2(2)	N(5)–C(17)–C(16)	118.7(2)
C(18)–C(17)–Li(1)	80.27(19)	N(5)–C(17)–Li(1)	60.55(17)
C(16)–C(17)–Li(1)	129.3(2)	C(17)–C(18)–Li(1)	67.69(18)

the nature of the azaallyl metal bonding does not have any significant bearing on the length of the (HMPA) O–Li bonds [*i.e.*, 1.855 Å (mean) in **3**, *cf.* 1.851 Å in **1**]. In displaying a η^3-NCC–Li bonding mode, the aforementioned silyl analogue [{$(Me_3Si)C(H)C(Bu^t)N(SiMe_3)Li$}$_2$] **4**[5] is more closely related to **3** than to **1**. Dimensions in **4** [N–Li, 1.97(1), 2.04(1); C–Li, 2.43(1), 2.44(1) Å] are similar to those in **3**, with the lack of a solvent–Li interaction being seemingly compensated for by a $Me_2SiMe\cdots Li$ agostic contact [distance to C, 2.48 (1) Å]. The aryl-substituted amidolithium [{Ph(Me)NLi·TMEN}$_2$][10] bears certain similarities to **1** since the C atoms of the NCC units avoid the metal centres of its $(NLi)_2$ dimeric ring; but the comparison is limited as its solvent molecule is didentate and so the Li coordination number is four not three [hence its (amide) N–Li bonds are longer (2.082 Å) than those in **1**].

Turning to the sodium azaallyl **2**, this is essentially an expanded version of the structure of **1** reflecting the larger size of Na^+ *cf.* Li^+. This increase in size enables two HMPA molecules to be accommodated within the metal coordination sphere [O–Na bond length, 2.2589(15) Å], rather than just one. The N terminus of the NCC unit bridges the symmetry-equivalent Na^+ cations in an asymmetrical manner (difference in bridge lengths, 0.04 Å); but the C atoms lie outside bonding range [C(17)$\cdots$Na(1), 3.472 Å; C(16)$\cdots$Na(1), 4.570 Å]. As in **1**, the *cis* conformation of the N–H and C–C bonds is accompanied by large obtuse CNNa bond angles (mean value, 131.31°). The structurally characterised 2-azaallyl complex [{PhC(H)NC(H)Ph}Na·PMDETA][11] provides a contrast with **2** as its N-anion can only bind terminally to the Na^+ cation because the steric bulk of the chelating amine helps to prevent dimerisation (PMDETA = *N*,*N*,*N*′,*N*″,*N*″-pentamethyldiethylenetriamine).

Considering the anion moieties on their own, an analysis of the bond lengths involved in the NCC units in **1**–**3** reveals only minor differences. Charge is delocalised essentially uniformly throughout, corresponding to a N⋯C⋯C representation intermediate between a metal–enamide and a metal–imidoalkyl. The change of ligating mode from η^1 to η^3 leads to a modest shortening of the N⋯C bond (by a mean of 0.029 Å from **1** to **3**), but there is no significant variation in the C⋯C bond lengths. However, the correlation between ligating mode and intra-ligand bond lengths is not simple, for in **4**, which exhibits η^3-ligation, the N⋯C bond length [1.402(7) Å] is closer to that in η^1-ligated **1**. Obviously the steric nature of the 'R' groups on the N and C termini, as well as solvation, must also influence how the ligand best fits the metal centre. Changing the solvated metal centre from $Li(HMPA)^+$ in **1** and **3** to $Na(HMPA)_2^+$ in **2** also has little effect on the dimensions of the N⋯C⋯C unit.

NMR spectroscopic studies

The three azaallyl complexes have also been characterised by ^{1}H and ^{13}C NMR spectroscopic studies in [$^2H_8$]toluene solution. From the former spectra it is clear that the azaallyl formulations found in the solid state are retained in solution: each spectrum displays a distinct N*H* signal and the α-CH_x unit bonded to the C⋯N bond exhibits the correct integral number of H atoms ($x = 1$ for **1** and **2**; $x = 2$ for **3**). In the case of **3**, one of these α-C*H* signals is split into a doublet through a long range coupling with the N*H* signal (^4J, 2.4 Hz), while the other α-C*H* signal remains a singlet. This example of "W-coupling"[12] confirms the "W" conformation observed in the crystal structure between the N*H* (1N and 5N) atoms and the α-C*H* (6B and 18B, respectively) atoms, which is a consequence of the *trans* orientation of the NH and C⋯C linkages. No such coupling is seen in the spectra of **1** and **2** which is consistent with the lack of a "W" conformation in the alternative *cis* arrangement displayed in their crystal structures. The only significant difference between the ^{1}H NMR spectra of **1** and **2** is the relative integral number of HMPA (1 and 2 molar equivalents, respectively); chemical shifts are generally similar for corresponding atoms, indicating that the amount of electron density and its distribution within the azaallyl skeleton is not affected to any great extent by the identity of the counter cation. The same can be said about the ^{13}C chemical shifts for **1** and **2**. Most significantly, their imido *C*⋯N signals appear at considerably lower frequencies (δ 165.54 and 167.93, respectively) than that in **3** (δ 174.25). This observation is in agreement with the shorter C⋯N bond found in the crystal structure of **3**, which signifies a slightly greater degree of imidoalkyl character.

Theoretical MO calculations

The lithium ketimide/lithium 1-azaallyl isomerism has been investigated by *ab initio* MO calculations[13] at the HF/6-31G* level.[14] The validity of each energy minimum structure was confirmed by performing a frequency analysis. For calculational simplicity we chose to model the methyl system of **3**, which is the most interesting experimental structure from the point of view of its η^3-NCC–Li bonding. Geometry optimisations of HMPA-free monomeric models revealed that the energy minimum structure of the azaallyl form $CH_2C(Bu^t)$-N(H)Li, **3A** (Fig. 4), is 3.9 kcal mol^{-1} more stable than that of its ketimido isomer $CH_3(Bu^t)$C=NLi, **3B** (Fig. 5) (this energy difference rises to 5.5 kcal mol^{-1} at the MP2 level[15]). Three-fold coordination of the lithium centre (*cf.* the single N–Li bond in **3B**) contributes to the greater stability of **3A**. This is accomplished by the ligand adopting a η^3-NCC bonding mode akin to that observed in the monomeric subunits of crystalline **3**, though the bond lengths involved are shorter (N–Li, 1.854, NC–Li, 2.150, NCC–Li, 2.135 Å; *cf.* mean values of **3**, 2.024, 2.366 and 2.521 Å, respectively), reflecting the absence of a donor ligand. Also as in **3**, the Li sits far out of the NCC ligand plane (the N–Li bond is inclined at an angle of 40.5° to this plane) and the N–H bond is disposed *trans* with respect to the delocalised C⋯C unit.

Calculation of **3A** with the N–Li *trans* to the delocalised C⋯C unit decreases the stability by 9.4 kcal mol^{-1} and this gives some indication of the magnitude of the Li–azaallyl interaction. The closer approach of the Li centre in **3A** results in a significant widening of the ligand bite angle [71.2° *cf.* 60.95° (mean) in **3**].

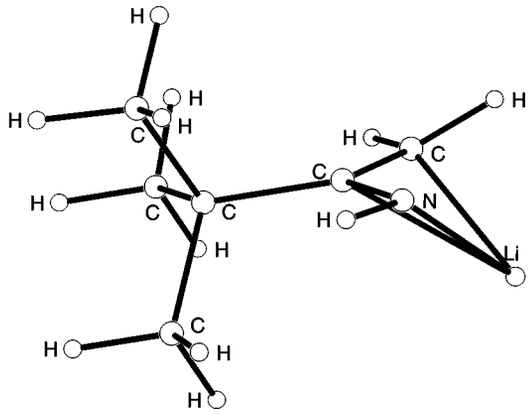

Fig. 4 HF/6-31G* geometry-optimised structure of azaallyl **3A**.

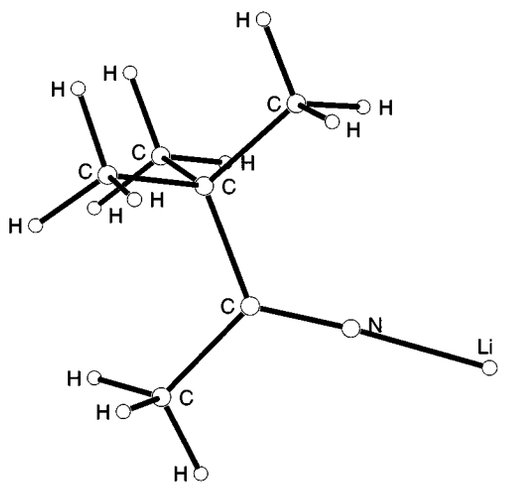

Fig. 5 HF/6-31G* geometry-optimised structure of ketimide **3B**.

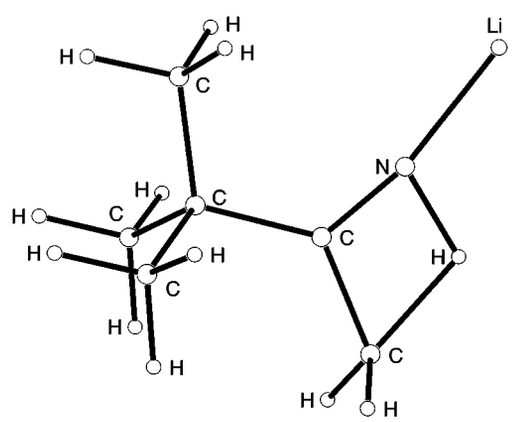

Fig. 6 HF/6-31G* geometry-optimised structure of the transition state **3C**.

Bond lengths within the NCC unit of **3A** (N···C, 1.333; C···C, 1.391 Å) suggest a uniform delocalisation of charge. This contrasts with the double and single bonds (lengths, 1.241 and 1.535 Å respectively) found within the N=C–C unit of the ketimide model **3B**. In this structure the C=N–Li unit is essentially linear (179°), and the N–Li bond is noticeably short (1.726 Å). Relevant to the hydrogen-transfer process, the closest N···H (Me) contact distance is 2.541 Å. To attempt to shed light on a possible intramolecular mechanism of this process the transition state between **3A** and **3B**, **3C** (Fig. 6), was calculated. Here the "moving" hydrogen takes up a bridging position between the methyl C atom and the N atom. By doing so, the N···H (Me) distance shortens to 1.256 Å (*cf.* the N–H bond length in **3A**, 0.998 Å), and the (H_2) C···H contact lengthens concomitantly from 1.082 (in **3B**) to 1.535 Å. This hydrogen

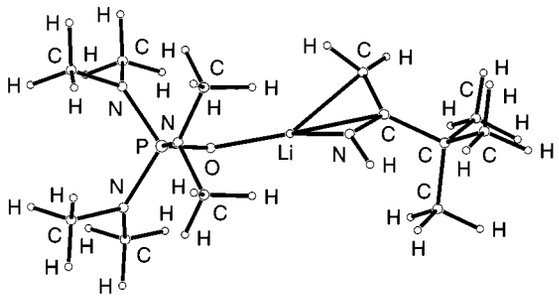

Fig. 7 HF/6-31G* geometry-optimised structure of the azaallyl **3A**·HMPA.

lies 1.629 Å from the central C atom of the NCC unit. Angles within the NCCH planar ring measure 80.2, 107.8, 64.7 and 107.2° at N,C,C and H respectively. The movement of the hydrogen has little bearing on the bond lengths within the N=C–C unit which measure 1.272 and 1.510 Å, respectively; but the N–Li bond lengthens to 1.770 Å and the CNLi bond angle narrows to 168.2°. Overall this structure is 77.5 kcal mol^{-1} higher in energy than **3A**, which corresponds to a formidable activation barrier of 73.6 kcal mol^{-1} (56.4 kcal mol^{-1} at MP2 level) for the conversion of **3B** to **3A** and effectively rules out an intramolecular transfer of this type.

The effect of solvation was considered by running calculations on HMPA complexes of the model monomers. Irrespective of the nature of the bonding within the anion, the addition of the strong oxygen donor was found to be a highly exothermic process as indicated in eqns. (4) and (5). This is as

$$CH_2C(Bu^t)N(H)Li + HMPA \longrightarrow CH_2C(Bu^t)N(H)Li\cdot HMPA \quad (4)$$
$$\Delta E_f = -29.1 \text{ kcal mol}^{-1}$$

$$CH_3(Bu^t)C{=}NLi + HMPA \longrightarrow CH_3(Bu^t)C{=}NLi\cdot HMPA \quad (5)$$
$$\Delta E_f = -33.0 \text{ kcal mol}^{-1}$$

expected since a new (HMPA) O–Li dative bond is created. The smaller stabilisation energy obtained for eqn. 4 reflects the greater bonding interaction of lithium with the azaallylic anion in the HMPA-free reactant. Less predictable, however, is that there is now no significant difference in the relative stability of the isomers: azaallylic **3A**·HMPA is only 0.08 kcal mol^{-1} more stable than the imide **3B**·HMPA.

The structure of the former solvate is shown in Fig. 7. This retains the η^3-NCC–Li chelation. Bond lengths involved (N–Li, 1.913, NC–Li, 2.223, NCC–Li, 2.255 Å) show a modest increase compared to those in **3A** due to the extra coordination by the solvent molecule. The N–Li bond is inclined at an angle of 43.8° to the NCC plane. There is good agreement between the O–Li bond length (1.861 Å) and that in the crystal structure of **3** (mean, 1.855 Å). The *trans* arrangement of the NH and C···C bonds is also maintained in **3A**·HMPA. Bond lengths within its NCC unit (N···C, 1.342; C···C, 1.376 Å) are not affected to any significant extent by the solvation. As in the case of the solvent-free models, a transition state (not shown) was calculated for the conversion of **3B**·HMPA to **3A**·HMPA. The activation energy was found to be +67.7 kcal mol^{-1}. This high value would clearly also rule out the possibility that proton transfer proceeds by a simple, one-step intramolecular process between two monomeric entities as was concluded in the case of **3A**. Of course, in reality, the experimental structure of **3** is dimeric. Calculations on the solvent-free dimer [{$CH_2C(Bu^t)$-N(H)Li}$_2$] (**3A**)$_2$ reveal that dimerisation is more favourable by 51.3 kcal (*i.e.*, by 25.7 kcal per mole of monomer). The dimer consists of two monomeric azaallyl units of **3A** joined together through a four membered Li–N–Li–N ring (Fig. 8). The two Li–N bonds which link the moieties span 1.960 Å and are shorter than the Li–N bond length present in each azaallyl unit

Table 4 Crystallographic data

Compound	**1**	**2**	**3**
Formula	$C_{30}H_{72}Li_2N_8O_2P_2$	$C_{42}H_{108}N_{14}Na_2O_4P_4$	$C_{24}H_{60}Li_2N_8O_2P_2$
M	652.8	1043.3	568.6
Crystal system	Monoclinic	Monoclinic	Monoclinic
Space group	$P2_1/n$	$P2_1/n$	$P2_1/c$
a/Å	11.6491(16)	10.6067(8)	23.163(2)
b/Å	13.930(2)	19.4806(14)	15.1740(14)
c/Å	12.2552(17)	15.1869(11)	10.1786(9)
β/°	90.013(3)	97.680(2)	101.871(2)
U/Å^3	1988.6(5)	3109.8(4)	3501.0(6)
T/K	160	160	160
Z	2	2	4
μ/mm^{-1}	0.14	0.18	0.16
Reflections measured	12296	19194	21473
Unique reflections	4669	7352	8260
R_{int}	0.0575	0.0406	0.0693
$wR2$ (F^2, all data)	0.1317	0.1132	0.1586
R (F, $F^2 > 2\sigma$)	0.0562	0.0456	0.0645

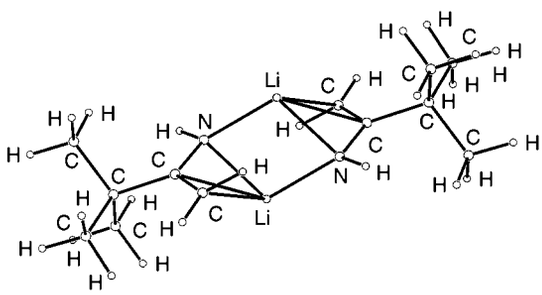

Fig. 8 HF/6-31G* geometry-optimised structure of the azaallyl dimer $(\mathbf{3A})_2$.

of 2.018 Å (*cf*. 1.854 Å in **3A**) (this mimics the pattern found in crystalline **3**). The lithium–carbon bond distances have also lengthened upon dimerisation to 2.272 and 2.296 Å as the lithium interacts with the second ring. The effect on the azaallyl of the second lithium coordinating to the N allows the CN bond to lengthen to 1.361 (from 1.333 in **3A**) and the C⋯C bond to shorten to 1.363 (from 1.391 Å in **3A**). These lengths are remarkably close to those determined from the X-ray diffraction study of **3** (Table 3). The lithium remains inclined to the N⋯C⋯C plane with a larger angle now of 47.0°.

Further calculations on solvated dimers and higher aggregates are currently in progress and will be reported at a later date.

Experimental

Preparations and characterisation

Reactions were carried out in Schlenk tubes under a protective atmosphere of dry, oxygen-free, argon. Commercial alkyllithium solutions (from Aldrich) were re-standardised before each application, using the diphenylacetic acid reagent–indicator method.[16] Sodium *tert*-butoxide was used as supplied. Bulk solvents were distilled from sodium–benzophenone, placed over fresh molecular sieves and covered by an argon blanket. HMPA and *tert*-butyl cyanide were dried over molecular sieves. NMR spectral data were recorded on a Bruker AMX 400 spectrometer or a Bruker DPX 400 spectrometer both operating at 400.13 MHz for ^{1}H.

Complex 1. Neat *tert*-butyl cyanide (10 mmol) was added dropwise to a chilled hexane solution of *n*-butyllithium (10 mmol) to afford a colourless solution with a pale green tinge. Allowed to warm up to room temperature, the solution was then treated with HMPA (10 mmol), which caused it to turn brown. Standing the solution for 24 h at room temperature yielded a crop of colourless, air-sensitive crystals of **1** (2.89 g, 80%), mp 78–79 °C (Found: C, 53.5; H, 11.2; N, 17.5; Li, 2.3; P, 9.5. $C_{15}H_{36}LiN_4OP$ requires C, 55.2; H, 11.0; N, 17.2; Li, 2.1; O, 4.9; P, 9.5%). ^{1}H NMR (400 MHz in [$^2H_8$]toluene, 298 K): δ 3.79 (t, 1H, α-C*H*), 2.38 (d, 18H, HMPA), 2.18 (br s, 1H, N*H*), 1.73 (sextet, 2H, γ-CH_2) 1.46 (s, 9H, Bu^t) and 1.21 (t, 3H, CH_3). ^{13}C NMR (100.6 MHz in [$^2H_8$]toluene, 298 K): δ 165.54 (*C*⋯N), 80.72 (α-*C*H), 36.90 (*C*(CH$_3$)$_3$), 36.63 (HMPA), 31.33–31.28 (β*C*H$_2$ + C(*C*H$_3$)$_3$), 25.00 (γ-*C*H$_2$) and 15.20 (*C*H$_3$).

Complex 2. *n*-Butylsodium was freshly prepared by reacting sodium *tert*-butoxide (15 mmol) with a hexane solution of *n*-butyllithium (15 mmol). Isolated by vacuum filtration as an off-white solid, the *n*-butylsodium (10 mmol) was suspended in hexane and chilled to 0 °C. To this was added *tert*-butyl cyanide (10 mmol), followed by two molar equivalents of HMPA (20 mmol). A dark brown solution was obtained on allowing the mixture to warm up to room temperature. Cooling this solution to 0 °C overnight afforded a crop of colourless, air-sensitive crystals of **2** (2.76 g, 53%), mp 90–92 °C (Found: C, 46.9; H, 10.2; N, 17.9; Na, 4.0; P, 11.9. $C_{21}H_{54}N_7NaO_2P_2$ requires C, 48.4; H, 10.4; N, 18.8; Na, 4.4; O, 6.1; P, 11.9%). ^{1}H NMR (400 MHz in [$^2H_8$]toluene, 298 K): δ 3.58 (t, 1H, α-C*H*), 2.43 (d, 36H, HMPA), 1.77 (sextet, 2H, γ-C*H*), 1.49 (s, 9H, Bu^t) and 1.26 (t, 3H, CH_3). ^{13}C NMR (100.6 MHz in [$^2H_8$]toluene, 298 K): 167.93 (*C*⋯N), 76.85 (α-*C*H), 37.67 (*C*(CH$_3$)$_3$), 37.17 (HMPA), 32.06–31.95 (β*C*H$_2$ + C(*C*H$_3$)$_3$), 25.64 (γ-*C*H$_2$) and 15.78 (*C*H$_3$).

Complex 3. Addition of *tert*-butyl cyanide (10 mmol) to a chilled solution of methyllithium (10 mmol) in diethyl ether gave a pale yellow solution, which was allowed to warm up to room temperature. HMPA (10 mmol) was then introduced to render the solution dark pink in colour. Standing the solution for 24 h at room temperature afforded a crop of colourless, air-sensitive crystals of **3** (1.61 g, 57%), mp 99–101 °C (Found: C, 50.2; H, 10.4; N, 18.2; Li, 2.5; P, 10.8. $C_{12}H_{30}LiN_4OP$ requires C, 50.7; H, 10.6; N, 19.7; Li, 2.5; O, 5.6; P, 10.9%). ^{1}H NMR (400 MHz in [$^2H_8$]toluene, 298 K): δ 3.57 (s, 1H, α-C*H*), 3.28 (d, ^4J 2.4 Hz, 1H, α-C*H′*), 2.61 (d, ^4J 2.4 Hz, N*H*), 2.40 (d, 18H, HMPA) and 1.44 (s, 9H, Bu^t). ^{13}C NMR (100.6 MHz in [$^2H_8$]toluene, 298 K): δ 174.25 (*C*⋯N), 62.64 (α-*C*HH′), 37.31 (*C*(CH$_3$)$_3$), 36.75 (HMPA) and 30.90 (C(*C*H$_3$)$_3$).

Crystal structure determination

Crystal data and other experimental information are given in Table 4. Methods and programs were as described previously.[17]

CCDC reference number 186/1128.

See http://www.rsc.org/suppdata/dt/1998/3431/ for crystallographic files in .cif format.

Acknowledgements

We thank the EPSRC for sponsoring this research and Dr R. Snaith (University of Cambridge) for useful discussion.

References

1 P. C. Andrews, D. R. Armstrong, M. MacGregor, R. E. Mulvey and D. Reed, *J. Chem. Soc.*, *Chem.Commun.*, 1989, 1341.
2 D. Stalke, M. Wedler and F. T. Edelmann, *J. Organomet. Chem.*, 1992, **431**, C1.
3 I. Cragg-Hine, M. G. Davidson, F. S. Mair, P. R. Raithby and R. Snaith, *J. Chem. Soc.*, *Dalton Trans.*, 1993, 2423.
4 M. S. Eisen and M. Kapon, *J. Chem. Soc.*, *Dalton Trans.*, 1994, 3507.
5 P. B. Hitchcock, M. F. Lappert and D.-S. Liu, *J. Chem. Soc.*, *Chem. Commun.*, 1994, 2637.
6 M. F. Lappert and D.-S. Liu, *J. Organomet. Chem.*, 1995, **500**, 203.
7 The monomeric structure of [{$(Me_3Si)_2C(C_6H_4Br\text{-}4)C(SiMe_3)N$}-Li·THF] has also been described in outline. See M. F. Lappert and M. Layh, *Tetrahedron Lett.*, 1998, **39**, 4745.
8 For other lithium azaallyl structures see R. I. Papasergio, B. W. Skelton, P. Twiss, A. H. White and C. L. Raston, *J. Chem. Soc.*, *Dalton Trans.*, 1990, 1161.
9 P. B. Hitchcock, M. F. Lappert and M. Layh, *J. Chem. Soc.*, *Dalton Trans.*, 1998, 1619.
10 D. Barr, W. Clegg, R. E. Mulvey, R. Snaith and D. S. Wright, *J. Chem. Soc.*, *Chem. Commun.*, 1987, 716.
11 P. C. Andrews, R. E. Mulvey, W. Clegg and D. Reed, *J. Organomet. Chem.*, 1990, **386**, 287.
12 H. Gunther, in *NMR Spectroscopy*, J. Wiley and Sons, Chichester, 1980, p. 115.
13 Gaussian 94 (Revision A.1), M. J. Frisch, G. W. Trucks, H. B. Schlegel, P. M. W. Gill, B. G. Johnson, M. A. Robb, J. R. Cheeseman, T. A. Keith, G. A. Petersson, J. A. Montgomery, K. Raghavachari, M. A. Al-Laham, V. G. Zakrzewski, J. V. Ortiz, J. B. Foresman, J. Cioslowski, B. B. Stefanov, A. Nanayakkara, M. Challacombe, C. Y. Peng, P. Y. Ayala, W. Chen, M. W. Wong, J. L. Andres, E. S. Replogle, R. Gomperts, R. L. Martin, D. J. Fox, J. S. Binkley, D. J. Defrees, J. Baker, J. P. Stewart, M. Head-Gordon, C. Gonzalez and J. A. Pople, Gaussian, Inc., Pittsburgh PA, 1995.
14 W. J. Hehre, R. Ditchfield and J. A. Pople, *J. Chem. Phys.*, 1972, **56**, 2257; P. C. Hariharan and J. A. Pople, *Theoret. Chim. Acta*, 1973, **28**, 213; J. D. Dill and J. A. Pople, *J. Chem. Phys.*, 1975, **62**, 2921.
15 C. Moller and M. S. Plesset, *Phys. Rev.*, 1934, **46**, 618.
16 W. G. Kofron and L. M. Baclawski, *J. Org. Chem.*, 1976, **41**, 1879.
17 C. Redshaw, V. C. Gibson, W. Clegg, A. J. Edwards and B. Miles, *J. Chem. Soc.*, *Dalton Trans.*, 1997, 3343.

Paper 8/05523H